Heterometallic Osmium−Mercury Chain Structures Linking Two $\{Os_3(CO)_{10}(\mu\text{-}X)\}$ Subunits (X = Cl, Br, I): Syntheses and Molecular Structures of $[\{Os_3(CO)_{10}(\mu\text{-}X)\}_2(\mu_4\text{-}Hg)]$ (X = Cl, I), $[\{Os_3(CO)_{10}(\mu\text{-}Cl)\}_2\{\mu\text{-}HgOs(CO)_4\}_2]$, and *cis*-$[Os(CO)_4\{(\mu\text{-}Hg)Os_3(CO)_{10}(\mu\text{-}Cl)\}_2]$

Yat-Kun Au and Wing-Tak Wong*

Department of Chemistry, The University of Hong Kong, Pokfulam Road, Hong Kong

Received September 6, 1996[⊗]

Treatment of RHgCl (R = Me, Et, Ph, Fc) with the activated cluster $[Os_3(CO)_{10}(NCMe)_2]$ produces the osmium−mercury mixed-metal clusters $[\{Os_3(CO)_{10}(\mu\text{-Cl})\}_2(\mu_4\text{-Hg})]$ (**1a**) and $[\{Os_3(CO)_{10}(\mu\text{-Cl})\}_2\{\mu\text{-HgOs}(CO)_4\}_2]$ (**2a**) in low yields. Cluster **1a** bears a central wingtip mercury atom simultaneously bridging two $\{Os_3(CO)_{10}(\mu\text{-Cl})\}$ units. Cluster **2a** comprises an unprecedented decanuclear osmium−mercury framework in which there is a central linear "Hg−$\{Os(CO)_4\}_2$−Hg" molecular backbone with the two $Os(CO)_4$ fragments arranged in a staggered conformation. Cluster **2a** is thermally unstable and converts slowly to *cis*-$[Os(CO)_4\{(\mu\text{-Hg})Os_3(CO)_{10}(\mu\text{-Cl})\}_2]$ (**4a**) *via* the extrusion of an $Os(CO)_4$ moiety under ambient conditions. Cluster **4a** comprises two $\{(\mu\text{-Hg})Os_3(CO)_{10}(\mu\text{-Cl})\}$ subcluster units bonded to a central $Os(CO)_4$ moiety in a *cis* configuration. Similar reactions with PhHgBr and MeHgI have also been investigated. Cluster **1a** crystallizes in the triclinic space group $P\bar{1}$ with $a = 9.112(2)$ Å, $b = 12.314(2)$ Å, $c = 15.501(4)$ Å, $\alpha = 84.92(2)°$, $\beta = 88.26(3)°$, $\gamma = 79.52(2)°$ and $Z = 2$. Cluster **2a** crystallizes in the triclinic space group $P\bar{1}$ with $a = 13.306(2)$ Å, $b = 20.768(5)$ Å, $c = 9.771(4)$ Å, $\alpha = 96.36(3)°$, $\beta = 90.50(2)°$, $\gamma = 98.81(2)°$ and $Z = 2$. Cluster **4a** crystallizes in the triclinic space group $P\bar{1}$ with $a = 18.356(2)$ Å, $b = 19.100(3)$ Å, $c = 14.478(2)$ Å, $\alpha = 89.783(2)°$, $\beta = 113.19(2)°$, $\gamma = 113.70(2)°$ and $Z = 4$.

Introduction

Organomercurials play an important role in the syntheses of osmium−mercury mixed-metal clusters of various nuclearities,[1−17] presumably because mercury atom can attach readily to a variety of main group and transition metal frameworks.[18−20] The polar osmium−mercury bonds in these compounds may trigger further chemical changes or core manipulations especially at the interface of different metallic domains. A representative example is the isolation and characterization of $[Os_{18}Hg_3C_2(CO)_{42}]^{2-}$ from which stepwise demercuriation of the central mercury atoms has yielded the complete series $[Os_{18}Hg_xC_2(CO)_{42}]^{y-}$ ($x = 1-3$, $y = 1-4$) *via* photochemical and redox chemical reactions.[3,13] Furthermore, interesting solution dynamics associated with the mercury fragments in a number of Os−Hg mixed-metal clusters have been reported.[9,15,19] Variable-temperature NMR investigations of clusters of the type $[\{M_3\}_2Hg]$ indicated that a μ_2-Hg bridging moiety possesses about the same mobility as a μ_2-hydrido ligand.[15] Despite these previous reports, attempts to synthesize new and novel Os−Hg mixed-metal frameworks still remain as one of the intensive area of research.

In this paper, we report the synthesis, characterization, and the associated structural rearrangement of a series of osmium−mercury carbonyl clusters derived from the reactions of alkyl- or arylmercury(II) halides (RHgX) with the activated triosmium cluster, $[Os_3(CO)_{10}(NCMe)_2]$.[21] Such attempts were conceived in analogy with the reactions between $[Os_3(CO)_{10}(NCMe)_2]$ and

* Author to whom correspondence should be addressed.
⊗ Abstract published in *Advance ACS Abstracts,* April 1, 1997.

(1) (a) Gade, L. H. *Angew. Chem., Int. Ed. Engl.* **1993**, 32. (b) Rosenberg, E.; Hardcastle, K. I. In *Comprehensive Organometallic Chemistry II*; Pergamon: London, 1995; Vol. 10, Chapter 6, p 323.
(2) Fajardo, M.; Holden, H. D.; Johnson, B. F. G.; Lewis, J.; Raithby, P. R. *J. Chem. Soc., Chem. Commun.* **1984**, 24. (b) Ragosta, J. M.; Burlitch, J. M. *Organometallics* **1986**, *5*, 1517; **1988**, *7*, 1469.
(3) (a) Gade, L. H.; Johnson, B. F. G.; Lewis, J.; McPartlin, M.; Powell, H. R. *J. Chem. Soc., Chem. Commun.* **1990**, 110. *J. Chem. Soc., Dalton Trans.* **1992**, 921. (b) Johnson, B. F. G.; Lewis, J.; McPartlin, M.; Scowen, I. J. *J. Chem. Soc., Dalton Trans.* **1996**, 597.
(4) Johnson, B. F. G.; Kwik, W. L.; Lewis, J.; Raithby, P. R.; Saharan, V. P. *J. Chem. Soc., Dalton Trans.* **1991**, 1037.
(5) Andren, P. L.; Cabeza, J. A.; Llamazares, A.; Riera, V.; Bois, C.; Jeannin, Y. *J. Organomet. Chem.* **1991**, *420*, 431.
(6) Zheng, Z.; Knobler, C. B.; Curtis, C. E.; Hawthorne, M. F. *Inorg. Chem.* **1995**, *34*, 432.
(7) Ceriotti, A.; Pergola, R. D.; Garlaschelli, L.; Manassero, M.; Masciocchi, N. *Organometallics* **1995**, *14*, 186.
(8) Gould, R. A. T.; Craighead, K. L.; Wiley, J. S.; Pignolet, L. H. *Inorg. Chem.* **1995**, *34*, 2902.
(9) Rosenberg, E.; Ryckman, D.; Hsu, I-Nan; Gellert, R. W. *Inorg. Chem.* **1986**, *25*, 194.
(10) Ermer, S.; King, K.; Hardcastle, K. I.; Rosenberg, E.; Lanfredi, A. M. M.; Tiripicchio, A.; Camellini, M. T. *Inorg. Chem.* **1983**, *22*, 1339.
(11) Braunstein, P.; Rose, J.; Tiripicchio, A.; Tiripicchio-Camellini, M. *J. Chem. Soc., Chem. Commun.* **1984**, 391. *J. Chem. Soc., Dalton Trans.* **1992**, 911.
(12) Charalambous, E.; Gade, L. H.; Johnson, B. F. G.; Kotch, T.; Lees, A. J.; Lewis, J.; McPartlin, M. *Angew. Chem., Int. Ed. Engl.* **1990**, *10*, 1137.
(13) Gade, L. H.; Johnson, B. F. G.; Lewis, L.; McPartlin, M.; Kotch, T.; Lees, A. J. *J. Am. Chem. Soc.* **1991**, *113*, 8698.
(14) Rosenberg, E.; Wang, J.; Gellert, R. W. *Organometallics* **1988**, *7*, 1093.
(15) Rosenberg, E.; Hardcastle, K. I.; Day, M. W.; Gobetto, R.; Hajela, S.; Muftikian, R. *Organometallics* **1991**, *10*, 203.
(16) Rossell, O.; Seco, M.; Segales, G.; Alvarez, S.; Pellinghelli, M. A.; Tiripicchio, A. *Organometallics* **1994**, *13*, 2205.
(17) Ragosta, J. M.; Burlitch, J. M. *J. Chem. Soc., Chem. Commun.* **1985**, 1187.
(18) Ferrer, M.; Perales, A.; Rossel, O.; Seco, M. *J. Chem. Soc., Chem. Commun.* **1990**, 1447.
(19) Bianchini, A.; Farrugia, L. J. *Organometallics* **1992**, *11*, 540.
(20) Li, J.; Rafferty, B. G.; Mulley, S.; Proerpio, D. M. *Inorg. Chem.* **1995**, *34*, 6417.
(21) For previous examples illustrating mercury−carbon bond cleavage, see: (a) Barbaro, P.; Cecconi, F.; Ghilardi, C. A.; Midollini, S.; Orlandini, A.; Vacca, A. *Inorg. Chem.* **1994**, *33*, 6163. (b) Garoufis, A.; Perlepes, S. P.; Schreiber, A.; Bau, R.; Hadjiliadis, N. *Polyhedron* **1996**, *15*, 177.

S0020-1669(96)01092-0 CCC: $14.00

the group 11 metal complexes $MPPh_3Cl$ (M = Cu, Ag, Au) in view of the fact that the $[R-Hg]^+$ fragment is isoelectronic (and isolobal) with [L−M] (L = neutral ligand such as PPh_3). While these isolobal fragments would sometimes lead to structurally similar mixed-metal products, their influence on the electronic (and thus geometrical) structures of the principal cluster cores may differ significantly.

Experimental Section

General Comments. All operations and reactions were carried out under an atmosphere of nitrogen using standard Schlenk techniques, unless otherwise indicated. Solvents were of reagent grade and were distilled from the appropriate drying agents and stored under nitrogen prior to use. Glassware was oven-dried at 140 °C. Products were isolated by preparative thin-layer chromatography (TLC) on silica gel (type 60) GF_{254} Merck 7730 in air.

Caution! Organomercurials are extremely toxic, and all experimentation involving these reagents should be carried out in a well-vented hood.

Instrumentation. All IR spectra were recorded on a BIO-RAD FTS-7 or SHIMADZU 470 IR spectrophotometer in CH_2Cl_2. ^1H (internal $SiMe_4$) and ^{199}Hg NMR (external 1 M phenylmercuric acetate in DMSO as secondary reference) were recorded in CD_2Cl_2 and $CDCl_3$, respectively, on a JEOL GSX 270 or Bruker DPX 300 FT-NMR spectrometers. Mass spectra were recorded on a Finnigan MAT 95 instrument using *m*-nitrobenzyl alcohol as the matrix. Electronic absorption spectra were obtained with a Hewlett Packard 8452A diode array UV/vis spectrophotometer. Elemental analyses were conducted by Butterworth Laboratories Ltd., London, U.K.

Reagents. $Os_3(CO)_{12}$, RHgCl (R = Me, Et, Ph), and MeHgI were purchased commercially (Strem) and used as received. Bromophenylmercury (PhHgBr),[22] (chloromercurio)ferrocene (FcHgCl),[23] and $[Os_3(CO)_{10}(NCMe)_2]$[24] were prepared according to the literature procedures.

Syntheses of $[\{Os_3(CO)_{10}(\mu\text{-Cl})\}_2(\mu_4\text{-Hg})]$ (1a) and $[\{Os_3(CO)_{10}(\mu\text{-Cl})\}_2\{\mu\text{-HgOs(CO)}_4\}_2]$ (2a). Solid $[Os_3(CO)_{10}(NCMe)_2]$ (50.0 mg, 0.05 mmol) dissolved in CH_2Cl_2 (20 mL) was added dropwise to a 5 mL CH_2Cl_2 solution of PhHgCl (22.0 mg, 0.07 mmol) over a period of 5 min. The resulting mixture was stirred for 1 h during which the color changed from pale yellow to blood red. The filtrate upon filtering off the precipitate was then reduced in volume under vacuum to 4 mL. Purification by preparative TLC using eluent hexane/CH_2Cl_2 (8:2 v/v) afforded two bands. The first dark purple band ($R_f \approx 0.65$) was $[\{Os_3(CO)_{10}(\mu\text{-Cl})\}_2(\mu_4\text{-Hg})]$ (**1a**). Dark purple crystals of **1a** suitable for single-crystal X-ray analysis were obtained from a CH_2Cl_2/hexane solution mixture on standing overnight under ambient conditions. Repeated TLC of the second orange band ($R_f \approx 0.45$) using eluent hexane/CH_2Cl_2 (9:1 v/v) afforded $[\{Os_3(CO)_{10}(\mu\text{-Cl})\}_2\{\mu\text{-HgOs(CO)}_4\}_2]$ (**2a**). Crystallization of **2a** from a $CHCl_3$/cyclohexane solution mixture afforded very thin orange plates. $[\{Os_3(CO)_{10}(\mu\text{-Cl})\}_2(\mu_4\text{-Hg})]$ (**1a**): Yield 27%. Anal. Calcd for $C_{20}Cl_2O_{20}HgOs_6$: C, 12.17. Found: 12.15. $[\{Os_3(CO)_{10}(\mu\text{-Cl})\}_2\{\mu\text{-HgOs(CO)}_4\}_2]$ (**2a**): Yield 8%. Anal. Calcd for $C_{28}Cl_2O_{28}Hg_2Os_8$: C, 12.10. Found: 12.28. Clusters **1a** and **2a** were also isolated when other organomercuric chlorides RHgCl (R = Me, Et, Fc) were used. Bromo analogs of clusters **1a** and **2a** (clusters **1b** and **2b**) and the corresponding iodo analogs (clusters **1c** and **2c**) were prepared by a similar procedure. $[\{Os_3(CO)_{10}(\mu\text{-Br})\}_2(\mu_4\text{-Hg})]$ (**1b**): Yield 32%. Anal. Calcd for $C_{20}Br_2O_{20}HgOs_6$: C, 11.65. Found: 11.71. $[\{Os_3(CO)_{10}(\mu\text{-Br})\}_2\{\mu\text{-HgOs(CO)}_4\}_2]$ (**2b**): Yield 12%. Anal. Calcd for $C_{28}Br_2O_{28}Hg_2Os_8$: C, 11.73. Found: C, 11.81. $[\{Os_3(CO)_{10}(\mu\text{-I})\}_2(\mu_4\text{-Hg})]$ (**1c**): Yield 38%. Anal. Calcd for $C_{20}I_2O_{20}HgOs_6$: C, 11.14. Found: 11.22. $[\{Os_3(CO)_{10}(\mu\text{-I})\}_2\{\mu\text{-HgOs(CO)}_4\}_2]$ (**2c**): Yield 10%. Anal. Calcd for $C_{28}I_2O_{28}Hg_2Os_8$: C, 11.35. Found: C, 11.38.

Synthesis of *cis*-$[Os(CO)_4\{(\mu\text{-Hg})Os_3(CO)_{10}(\mu\text{-Cl})\}_2]$ (4a). A solution of cluster **2a** (50 mg, 0.02 mmol) in freshly distilled THF (20 mL) was heated to reflux under nitrogen. The reaction was monitored by IR (carbonyl stretching frequency) and was completed after 10 h.

Scheme 1. Formation of **1a**, **2a**, and **4a**[a]

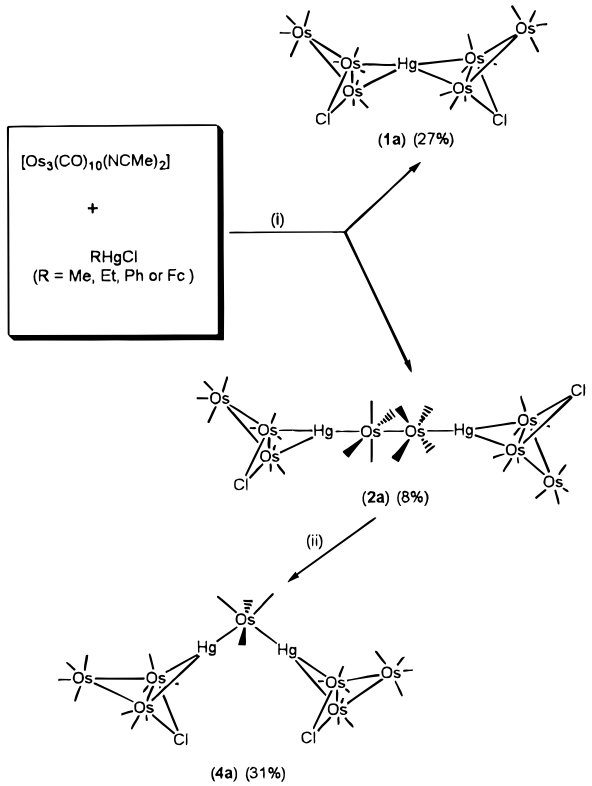

[a] (i) CH_2Cl_2, 1 h; (ii) THF, 10 h.

The solvent was then removed under reduced pressure, and the residue was redissolved in CH_2Cl_2 (3 mL). TLC separation using the eluent hexane/CH_2Cl_2 (9:1 v/v) gave the orange cluster *cis*-$[Os(CO)_4\{(\mu\text{-Hg})Os_3(CO)_{10}(\mu\text{-Cl})\}_2]$ (**4a**) ($R_f \approx 0.5$) as the major product. Dark orange crystals of cluster **4a** suitable for X-ray analysis were obtained from a CH_2Cl_2 solution of cluster **4a** under ambient conditions over a period of 1 week. *cis*-$[Os(CO)_4\{(\mu\text{-Hg})Os_3(CO)_{10}(\mu\text{-Cl})\}_2]$ (**4a**): Yield 31%. Anal. Calcd for $C_{24}Cl_2O_{24}Hg_2Os_7$: C, 11.63. Found: C, 11.71. The respective bromo and iodo analogs of **4a**, clusters **4b**,**c**, were prepared by a similar procedure. *cis*-$[Os(CO)_4\{(\mu\text{-Hg})Os_3(CO)_{10}(\mu\text{-Br})\}_2]$ (**4b**): Yield 27%. Anal. Calcd for $C_{24}Br_2O_{24}Hg_2Os_7$: C, 11.23. Found: C, 11.37. $[Os(CO)_4\{(\mu\text{-Hg})Os_3(CO)_{10}(\mu\text{-I})\}_2]$ (**4c**): Yield 35%. Anal. Calcd for $C_{24}I_2O_{24}Hg_2Os_7$: C, 10.83. Found: C, 10.91.

Crystal Structure Analyses of 1a, 2a, and 4a. Single crystals suitable for X-ray analysis were mounted on a glass fiber (**1a** and **4a**) or in a Lindermann glass capillary (**2a**) using epoxy resin. Unit cell constants of each compound were determined from a least-squares analysis of the setting angles of 25 accurately centered reflections with 2θ values in the range 16−24°. Intensity data were collected at ambient temperature on either an Enraf-Nonius CAD4 (for **1a** and **4a**) or a Riguka AFC7R (for **2a**) diffractometer using graphite monochromated Mo Kα radiation (λ = 0.710 73 Å) with an $\omega-2\theta$ scan technique. A summary of pertinent crystallographic, structure solution, and refinement data is listed in Table 5. Monitoring of three standard reflections at an interval of 2 h throughout the data collection showed no sign of crystal deterioration for crystals **1a** and **4a**. However, a significant decay (36%) was encountered for crystal **2a**. Therefore, a linear decay correction was applied for **2a**. Lorentz−polarization and ψ-scan absorptions were applied to all the intensity data.[25] Neutral atom scattering factors were taken from ref 26a, and anomalous dispersion effects[26b] were included in F_c.

Space groups of all crystals were determined from a Laue symmetry check and their systematic absences and confirmed by successful

(22) Hill, E. L. *J. Am. Chem. Soc*. **1928**, *50*, 167.
(23) Fish, R. W. *J. Org. Chem*. **1957**, *22*, 960.
(24) Nicholls, J. N.; Vargas, M. D. *Inorg. Synth*. **1989**, *28*, 232.
(25) North, A. C. T.; Phillips, D. C.; Mathews, F. S. *Acta Crystallogr*. **1968**, *A24*, 351.
(26) Cromer, D. T.; Waber, J. T. *International Tables for X-Ray Crystallography*; Kynoch Press: Birmingham, U.K., 1974; Vol. 4: (a) Table 2.2B; (b) Table 2.3.1.

Table 1. Spectroscopic Data for **1**, **2**, and **4** (**a**−**c**)

cluster	IR: ν(CO)[a] cm^{-1}	^{199}Hg NMR:[b] δ (ppm)	MS: M^{+} [d] (*m*/*z*)	λ_{max}[e]/nm (ϵ/dm^3 mol^{-1} cm^{-1})
1a	2113 (w), 2102 (m), 2063 (vs), 2028 (s), 2017 (s), 1996 (m,br)	−441	1977 (1977)	528 (2191)
2a	2105 (s), 2096 (s), 2059 (vs), 2022 (s), 2000 (s), 1976 (m)	−755	2782 (2782)	476 (4792)
4a	2105 (m), 2079 (m), 2060 (vs), 2023 (s), 2004 (m), 1972 (w)	−599	2478 (2478)	486 (3105)
1b	2113 (w), 2101 (m), 2061 (vs), 2025 (m), 2018 (s), 1993 (m)	*c*	2066 (2066)	510 (2564)
2b	2104 (m), 2096 (m), 2057 (vs), 2022 (s), 1998 (s), 1973 (m)	−895	2869 (2869)	455 (3277)
1c	2111 (w), 2099 (m), 2057 (vs), 2018 (s) 1989 (m)	−926	2160 (2160)	486 (2985)
2c	2103 (m), 2095 (m), 2054 (vs), 2021 (s), 1997 (s), 1972 (m)	−996	2963 (2963)	436 (2399)
4b	2104 (m), 2078 (w), 2057 (vs), 2021 (s), 2001 (m),1973 (w)	*c*	2567 (2567)	462 (2768)
4c	2102 (m), 2077 (w), 2055 (vs), 2021 (s), 1999 (m), 1972 (w)	*c*	2661 (2661)	441 (1963)

[a] vs = very strong, s = strong, m = medium, w = weak, br = broad. In CH_2Cl_2. [b] Versus Me_2Hg, assuming δ for PhHg(OAc) (1 M in DMSO) to be −1437 ppm at 25 °C. [c] No signal detected at 25 °C. [d] Calculated value in parentheses. [e] Measured in CH_2Cl_2 at 25 °C.

refinement of the structures. The structures were solved by a combination of direct methods (SIR 88)[27] and difference Fourier techniques. Refinement was carried out by full-matrix least-squares analysis with anisotropic displacement parameters for non-hydrogen atoms, if possible. Final difference Fourier maps revealed no significant feature in all the structures. All calculations were performed on a Silicon-Graphics workstation using the TEXSAN software package.[28]

Results and Discussion

Preparation and Structural Characterization of [{Os_3-(CO)$_{10}$(μ-Cl)}$_2$(μ_4-Hg)] (1a) and [{Os_3(CO)$_{10}$(μ-Cl)}$_2${μ-HgOs(CO)$_4$}$_2$] (2a). The reaction of [Os_3(CO)$_{10}$(NCMe)$_2$] with 1 equiv of PhHgCl produced **1a** and **2a** in low yields (Scheme 1). The infrared ν(CO) absorption band pattern of **1a** resembles those of the Os−Hg clusters previously prepared such as [{Os_3-(CO)$_{10}$(μ-η^2-CH=CHPh)}(μ_4-Hg)][29] with the bands of **1a** shifted to higher wavenumbers by about 10 cm^{-1} (Table 1). This may be attributed to the electronegative chlorine atoms in the cluster core of **1a**. A single-crystal X-ray analysis of **1a** was carried out in order to establish its molecular structure.

A perspective drawing of **1a** is depicted in Figure 1; important bond parameters are presented in Table 2. The molecular structure reveals a heptametallic Os−Hg metal cluster framework, consisting of two metal butterflies [Os(1), Os(2), Os(3), and Hg(1)] and [Os(4), Os(5), Os(6), and Hg(1)] sharing a common wingtip Hg(1) atom. The average dihedral angle of each butterfly unit is 52.0(2)°. These two metal butterflies are arranged in the cisoid configuration but are skewed. Thus the dihedal angle between the Os(1)−Hg(1)−Os(2) and Os(4)−Hg(1)−Os(5) planes is 39.4°, which is close to that in [{Ru_3-(CO)$_9$(μ_3-ampy)}$_2$(μ_4-Hg)][5] (ampy = 2-aminopyridine) but is much diminished compared to that measured in [{Os_3(CO)$_9$(μ-H)(μ_3-S)}$_2$(μ_4-Hg)][15] (65.0°). The skewing is inferred from the non-bonding interaction between the carbonyl ligands on Os(1) and Os(5) and on Os(2) and Os(4), and such a geometry tends to minimize this interaction. In the osmium triangles, the Os−Os vector doubly-bridged by the bridgehead chlorine atom and the mercury atom is slightly longer than the other two unsupported Os−Os bonds [e.g. Os(1)−Os(2), 2.867(1); Os(2)−Os(3), 2.830(1); Os(1)−Os(3), 2.843(1) Å]. The same pattern was also encountered in [Os_3(CO)$_{10}$(μ-H)(μ-Cl)][30] and [Os_3(CO)$_{10}$(μ-AuPPh$_3$)(μ-Cl)],[31] and such a lengthening is ascribed to the larger sizes of the bridgehead mercury and chlorine atoms.

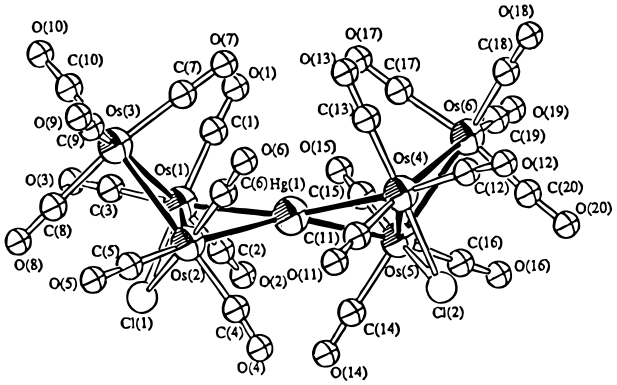

Figure 1. Perspective view of [{Os_3(CO)$_{10}$(μ-Cl)}$_2$(μ_4-Hg)] (1a).

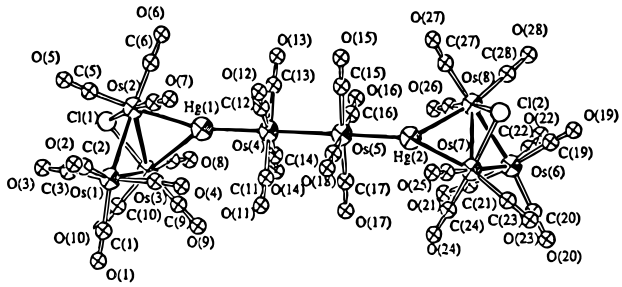

Figure 2. Perspective view of [{Os_3(CO)$_{10}$(μ-Cl)}$_2${μ-HgOs(CO)$_4$}$_2$] (2a).

Table 2. Selected Bond Lengths (Å) and Angles (deg) for **1a**

Os(1)−Os(2)	2.867(1)	Os(4)−Os(5)	2.868(1)
Os(1)−Os(3)	2.843(1)	Os(4)−Os(6)	2.836(2)
Os(2)−Os(3)	2.830(1)	Os(5)−Os(6)	2.843(2)
Os(1)−Hg(1)	2.857(1)	Os(4)−Hg(1)	2.859(1)
Os(2)−Hg(1)	2.837(1)	Os(5)−Hg(1)	2.822(1)
Os(1)−Os(3)−Os(2)	60.72(2)	Os(4)−Os(6)−Os(5)	60.68(2)
Os(1)−Os(2)−Os(3)	59.86(2)	Os(4)−Os(5)−Os(6)	59.55(3)
Os(2)−Os(1)−Os(3)	59.42(2)	Os(5)−Os(4)−Os(6)	59.77(3)
Os(1)−Hg(1)−Os(2)	60.46(2)	Os(4)−Hg(1)−Os(5)	60.65(2)
Os(1)−Hg(1)−Os(4)	164.82(3)	Os(2)−Hg(1)−Os(4)	121.57(3)
Os(1)−Hg(1)−Os(5)	124.57(3)	Os(2)−Hg(1)−Os(5)	156.21(3)

The molecular structure for **2a** is shown in Figure 2; important bond parameters are given in Table 3. The structure reveals an unprecedented decanuclear Os−Hg mixed-metal framework in which a central linear "Hg−{Os(CO)$_4$}$_2$−Hg" moiety is sandwiched between two {Os_3(CO)$_{10}$(μ-Cl)} triosmium units. The osmium−mercury domains [Os(1)−Os(2)−Os(3)−Hg(1); Os(6)−Os(7)−Os(8)−Hg(2)] are structurally very similar, and if we disregard the central −{Os(CO)$_4$}$_2$− units, the two

(27) Burla, M. C.; Camalli, M.; Cascarano, G.; Giacovazzo, C.; Polidori, G.; Spagna, R.; Viterbo, D. *J. Appl. Crystallogr*. **1989**, *22*, 389.
(28) TEXSAN: Crystal Structure Analysis Package, Molecular Structure Corp., Houston, TX, 1985 and 1992.
(29) Au, Y. K.; Wong, W. T. *J. Chem. Soc., Dalton Trans*. **1996**, 899.
(30) Churchill, M. R.; Lachewycz, R. A. *Inorg. Chem*. **1982**, *21*, 1707.
(31) Hay, C. M. Ph.D. Thesis, University of Cambridge, 1987.

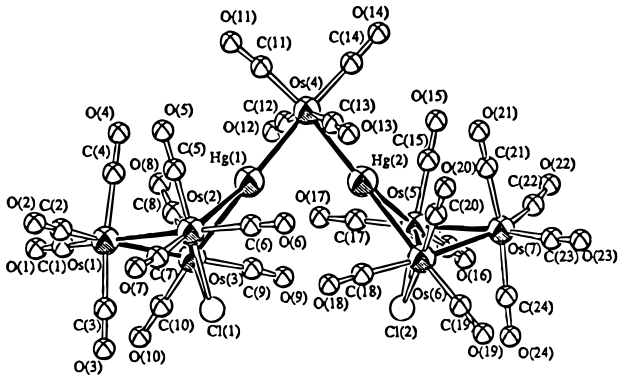

Figure 3. Perspective view of *cis*-$[Os(CO)_4\{(\mu\text{-}Hg)Os_3(CO)_{10}(\mu\text{-}Cl)\}_2]$ (4a).

Table 3. Selected Bond Lengths (Å) and Angles (deg) for **2a**

Os(1)−Os(2)	2.856(2)	Os(6)−Os(7)	2.862(2)
Os(1)−Os(3)	2.845(2)	Os(6)−Os(8)	2.840(3)
Os(2)−Os(3)	2.902(2)	Os(7)−Os(8)	2.889(2)
Os(2)−Hg(1)	2.823(2)	Os(7)−Hg(2)	2.823(2)
Os(3)−Hg(1)	2.832(2)	Os(8)−Hg(2)	2.823(2)
Hg(1)−Os(4)	2.645(2)	Hg(2)−Os(5)	2.650(2)
Os(4)−Os(5)	2.903(2)		
Os(1)−Os(2)−Os(3)	59.23(5)	Os(6)−Os(7) -Os(8)	59.19(6)
Os(1)−Os(3)−Os(2)	59.58(5)	Os(6)−Os(8)−Os(7)	59.93(6)
Os(2)−Os(1)−Os(3)	61.19(5)	Os(7)−Os(6)−Os(8)	60.88(6)
Os(2)−Hg(1)−Os(3)	61.74(5)	Os(7)−Hg(2)−Os(8)	61.54(5)

triosmium units are arranged in a skewed transoid configuration with the average dihedral angle of the Os−Hg butterflies being 57.03(2)°.

A salient structural feature of **2a** is the central linear Hg(1)−Os(4)−Os(5)−Hg(2) metal skeleton. The linear geometry of the "metal rod" is manifested in the angles of Hg(1)−Os(4)−Os(5) [179.58(7)°] and Os(4)−Os(5)−Hg(2) [178.97(7)°]. Both of the central Os atoms [Os(4), Os(5)] assume a pseudo-octahedral configuration, and the atoms of each set of four carbonyl ligands bonded respectively to Os(4) and Os(5) are essentially coplanar and offset in a staggered conformation. Consequently, the bonding interaction between the filled d_π orbitals of either osmium atom and the equatorial CO's π^* antibonding orbitals on their respective adjacent Os atoms is maximized [32] while the nonbonding interaction between the carbonyls is minimized. The central Os(4)−Os(5) distance [2.903(2) Å] is close to that observed in the linear cluster $[Os_3(CO)_{12}I_2]$[33] [2.935(2) Å] but is slightly longer than the average Os−Os distance of 2.877(3) Å in $[Os_3(CO)_{12}]$.[34]

The novel Os−Hg metal core of 2**a** demonstrates the ability of Hg atom to act as a "linker" in metal chain structures. In fact, the metal domain may be viewed as an extension of the type of linkage found in *cis*-$[Os(CO)_4\{(\mu\text{-}Hg)Os_3(CO)_{10}(\mu\text{-}\eta^2\text{-}CH{=}CHPh)\}_2]$ (**3**)[29] and **4a** (*vide infra*) in which two triosmium units are linked by a zigzag Hg−Os−Hg chain. The group 8 transition metal [M = Fe, Ru, Os] carbonyl fragments "$M(CO)_4$" acting as individual linking units have been previously found in $[Hg\{Fe(CO)_4(\mu\text{-}Hg)Fe_3(\mu\text{-}COMe)(CO)_{10}\}_2]$,[19] *cis*-$[Ru(CO)_4\{(\mu\text{-}Hg)Ru_3(CO)_9(\mu_3\text{-}C_2\text{-}t\text{-}Bu)\}_2]$,[9] $[Os_3\{\mu\text{-}AuOs(CO)_4(PPh_3)\}(\mu\text{-}Cl)(CO)_{10}]$,[35] and cluster **3**.

Synthesis and Structural Characterization of *cis*-$[Os(CO)_4\{(\mu\text{-}Hg)Os_3(CO)_{10}(\mu\text{-}Cl)\}_2]$ (4a). Cluster **2a** undergoes slow conversion to **4a** in solution under ambient conditions (see Experimental Section). Single-crystal X-ray analysis of **4a** revealed two crystallographically independent, but very similar, molecules within an asymmetric unit. A perspective view of molecule 1 is shown in Figure 3. Pertinent bonding parameters of both molecules are summarized in Table 4. (Hereafter all bonding parameters refer to those of molecule 1.) The structure consists of a central $Os(CO)_4$ fragment bound to two $\{(\mu\text{-}Hg)Os_3(CO)_{10}(\mu\text{-}Cl)\}$ units in a *cis* configuration. The geometry around Os(4) is a distorted octahedron; the Hg(1)−Os(4)−Hg(2) angle is 84.35(4),° and the Hg(1)−Os(4)−C(12) angle is 81.6(9).° The Hg(1)−Os(4)−Hg(2) angle and the intramolecular Hg···Hg distance of 3.60 Å suggest that a weak Hg···Hg interaction exists.[1b]

Table 4. Selected Bond Lengths (Å) and Angles (deg) for **4a**

molecule 1		molecule 2	
Os(1)−Os(2)	2.845(2)	Os(8)−Os(9)	2.838(2)
Os(1)−Os(3)	2.840(2)	Os(8)−Os(10)	2.836(2)
Os(2)−Os(3)	2.892(2)	Os(9)−Os(10)	2.894(2)
Os(5)−Os(6)	2.895(2)	Os(12)−Os(13)	2.890(2)
Os(5)−Os(7)	2.832(2)	Os(12)−Os(14)	2.840(2)
Os(6)−Os(7)	2.843(2)	Os(13)−Os(14)	2.842(2)
Hg(1)−Os(2)	2.832(1)	Hg(3)−Os(9)	2.834(2)
Hg(1)−Os(3)	2.830(2)	Hg(3)−Os(10)	2.821(2)
Hg(1)−Os(4)	2.682(1)	Hg(3)−Os(11)	2.674(2)
Hg(2)−Os(5)	2.820(2)	Hg(4)−Os(12)	2.962(2)
Hg(2)−Os(6)	2.817(2)	Hg(4)−Os(13)	2.828(2)
Hg(2)−Os(4)	2.675(2)	Hg(4)−Os(11)	2.693(2)
Os(2)−Os(1)−Os(3)	61.15(4)	Os(9)−Os(8)−Os(10)	61.34(4)
Os(1)−Os(2)−Os(3)	59.35(4)	Os(8)−Os(10)−Os(9)	59.36(4)
Os(1)−Os(3)−Os(2)	59.50(4)	Os(8)−Os(9)−Os(10)	59.30(4)
Os(2)−Hg(1)−Os(3)	61.43(4)	Os(9)−Hg(3)−Os(10)	61.56(4)
Os(5)−Os(7)−Os(6)	61.35(4)	Os(12)−Os(14)−Os(13)	61.15(4)
Os(6)−Os(5)−Os(7)	59.51(4)	Os(13)−Os(12)−Os(14)	59.45(4)
Os(5)−Os(6)−Os(7)	59.14(4)	Os(12)−Os(13)−Os(14)	59.40(4)
Os(5)−Hg(2)−Os(6)	61.81(4)	Os(12)−Hg(4) -Os(13)	61.05(4)
Hg(1)−Os(4)−Hg(2)	84.35(4)		

Table 5. Crystallographic Data for **1a**, **2a** and **4a**[a]

	1a	**2a**	**4a**
empirical formula	$C_{20}Cl_2HgO_{20}Os_6$	$C_{34}Cl_2H_{12}Hg_2O_{28}Os_8$	$C_{24}Cl_2Hg_2O_{24}Os_7$
M_r	1972.91	2862.14	2478.74
cryst system	triclinic	triclinic	triclinic
space group	$P\bar{1}$ (No. 2)	$P\bar{1}$ (No. 2)	$P\bar{1}$ (No. 2)
a/Å	9.112(2)	13.306(2)	18.356(2)
b/Å	12.314(2)	20.768(5)	19.100(3)
c/Å	15.501(4)	9.771(4)	14.478(2)
α/deg	84.92(2)	96.36(3)	89.783(2)
β/deg	88.26(3)	90.50(2)	113.19(2)
γ/deg	79.52(2)	98.81(2)	113.70(2)
V/Å^3	1716.3(1)	2651(1)	4198(1)
Z	2	2	4
ρ_{calcd}/g cm^{-1}	3.817	3.585	3.914
μ/cm^{-1}	268.44	250.40	285.75
temp/°C	25	25	25
λ/Å	0.710 73	0.710 73	0.710 73
R^b	0.031	0.043	0.034
$R_w{}^c$ (obsd data)	0.038	0.043	0.046
goodness of fit, S	1.21	1.62	1.64

[a] Weighting scheme = $1/\sigma^2(|F_o|)$. [b] $R = \sum||F_o| - |F_c||/\sum|F_o|$ [c] $R_w = [\sum w(|F_o| - |F_c|)^2/\sum wF_o^2]^{1/2}$.

Core Transformation from 2a to 4a. The overall transformation involves extrusion of a mononuclear $Os(CO)_4$ fragment, together with a stereochemical change at the remaining osmium atom from a *trans* to a *cis* configuration, and has been monitored by IR and UV−vis spectroscopies. During the process there is a smooth decrease in intensity of the ν(CO) band in the IR spectrum at 2096 cm^{-1} and the concomitant appearance of a band centered at 2079 cm^{-1} while a decline in intensity of the absorption band at 476 nm and a bathochromic

(32) Bau, R.; Kirtley, S. W.; Sorrell, T. N.; Winarko, S. *J. Am. Chem. Soc*. **1974**, 988.
(33) Cook, N.; Smart, L.; Woodward, P. *J. Chem. Soc., Dalton Trans*. **1977**, 1744.
(34) Churchill, M. R.; Deboer, B. G. *Inorg. Chem*. **1977**, *16*, 878.
(35) Cathey, C. J.; Lewis, J.; Raithby, P. R.; Carmen Ramirez de Arellano, M. *J. Chem. Soc., Dalton Trans.* **1994**, 3331.

shift to 486 nm was observed in the corresponding UV−vis spectrum (Table 1). Absorption bands in this energy range may be attributable to transitions between orbitals involved in the metal−metal bonds within the cluster core. Since the structural changes that go along with the transformation are primarily confined to the central Os−Hg frame, we believe that the absorption band arises from the metal-centered charge-transfer transition to the antibonding orbitals[36] associated with these Os−Hg and Os−Os bonds but not the corresponding counterparts of the Os_3 triangles. There is no isosbestic point associated with the transformation, and therefore, the conversion is not likely to be a one-step process.

Reactions with Other RHgX Reagents (R = Me, Et, Ph, Fc; X = Cl, Br, I). Reactions of $[Os_3(CO)_{10}(NCMe)_2]$ with RHgCl (R = Me, Et, Fc) have also been carried out where the R groups possess different degrees of electron-donating ability. Spectroscopic results indicates that, in each case, **1a** and **2a** are formed as the major products. However, the reaction rates follow the order Fc > Et > Me under identical experimental conditions. Similar attempts but employing PhHgBr and MeHgI have been undertaken. As expected, the bromo and iodo analogs of **1a** (**1b**,**c**) and **2a** (**2b**,**c**) can also be isolated. In these cases, however, there was no dependence of the observed reaction rates on the identity of the halides.

Concluding Remarks

A series of high-nuclearity osmium−mercury metal carbonyl clusters have been synthesized from the reaction between $[Os_3(CO)_{10}(NCMe)_2]$ and organomercurials RHgX (X = Cl, Br, I). The new clusters $[\{Os_3(CO)_{10}(\mu\text{-}X)\}_2(\mu_4\text{-}Hg)]$, $[\{Os_3(CO)_{10}(\mu\text{-}X)\}_2\{\mu\text{-}HgOs(CO)_4\}_2]$, and *cis*-$[Os(CO)_4\{(\mu\text{-}Hg)Os_3(CO)_{10}(\mu\text{-}X)\}_2]$ (X = Cl, Br, I) are found to consist of a central "Hg", "Hg−$\{Os(CO)_4\}_2$−Hg" , and "*cis*-Hg−$Os(CO)_4$−Hg" linker, respectively bridging two $\{Os_3(CO)_{10}(\mu\text{-}X)\}$ units.

Scheme 2. Redistribution Reaction of $[Os_3(CO)_{10}(\mu\text{-}X)(\mu\text{-}HgR)]$ (X = halides; R = Alkyl, Aryl)

$$2\,[Os_3(CO)_{10}(\mu\text{-}X)(\mu\text{-}HgR)] \rightleftharpoons [\{Os_3(CO)_{10}(\mu\text{-}X)\}_2(\mu_4\text{-}Hg)] + HgR_2 \quad (1)$$

A sensible interpretation of this reaction chemistry is that oxidative addition of the mercury−halogen bonds of the RHgX to the triosmium core is an essential step based on previous studies.[1b] The asymmetric mercurial, $[Os_3(CO)_{10}(\mu\text{-}X)(\mu\text{-}HgR)]$, is produced which redistributes rapidly to produce $[\{Os_3(CO)_{10}(\mu\text{-}X)\}_2(\mu_4\text{-}Hg)]$ (**1a,b,c**) and HgR_2 (Scheme 2) since symmetrization is favored when there is an organic group (R = alkyl, aryl) attached to the mercury atom.[1b] Indeed, the observed variation of the reaction rates for different R groups could well be rationalized by the differences in the rates of the respective redistribution reactions. Although significant amount of HgR_2 cannot be isolated by a chromatographic method to support this argument, this may due to the fact that decomposition of $[Os_3(CO)_{10}(\mu\text{-}X)(\mu\text{-}HgR)]$ to **1**, R−R, and metallic mercury is also significant. Nevertheless, our present results establish new examples of Hg−C bond cleavage[21] and highlight that organomercurials play an important role in the synthesis of high-nuclearity mixed-metal framework.

Acknowledgment. W.-T.W. acknowledges the financial support from the Hong Kong Research Grants Council and The University of Hong Kong. Y.-K.A. thanks the receipt of a postgraduate studentship and a Hung Hing Ying Scholarship, administered by The University of Hong Kong.

Supporting Information Available: Complete listings of crystallographic data and structure solution, final atomic coordinates, anisotropic displacement parameters, and intramolecular bond distances and bond angles and ORTEP diagrams for **1a**, **2a**, and **4a** (28 pages). Ordering information is given on any current masthead page.

IC961092P

(36) Gladfelter, W. L.; Geoffroy, G. Y. *Adv. Organomet. Chem.* **1980**, *18*, 207.